Conductance quantization in nanowires formed between micro and macroscopic metallic electrodes

J. L. Costa-Krämer, N. García, P. García-Mochales, P. A. Serena, M. I. Marqués, and A. Correia
Laboratorio de Física de Sistemas Pequeños (CSIC-UAM), Universidad Autónoma de Madrid, C-IX, Cantoblanco, E-28049-Madrid, Spain

(Received 16 November 1995; revised manuscript received 4 October 1996)

In this work we present experimental results concerning conductance quantization at room temperature in metallic nanowires. The experiments are performed both at ambient presure and in ultrahigh vacuum using scanning tunneling microscopy (STM)-like devices. Both microscopic and macroscopic electrodes are used. The obtained results are independent of the electrode size, indicating that nanowires form at the last stages of the contact-breakage process, independently of the initial size and shape of the contact. In addition, we study (a) the stability of the nanowires, finding their lifetimes remarkably long, on the order of minutes; (b) the *I-V* curves for different quantum channels; (c) nanowires formed and visualized using a STM inside a scanning electron microscope (SEM); (d) the statistical behavior of the conductance, sampling tens of thousands of consecutive conductance experiments, showing clear quantized peaks up to five quanta of conductance; and (e) the length of the conductance plateaus, that might indicate the chaotic behavior of the quantum states formed at the nanowire. The statistical study of the conductance plateau lengths shows a broad Wigner-like distribution with an average value of 0.13 nm for the first quantum channel. This is at variance with a constant length, predicted and experimentally observed, in the plateaus between force jumps. [S0163-1829(97)00207-5]

I. INTRODUCTION

The conductance through a small constriction in a two-dimensional electron gas (2DEG) is quantized[1] when its width varies, being the quantum of conductance $G_0=2e^2/h$, where e is the electron charge and h the Planck constant. The study of electronic transport through small metallic and nonmetallic contacts has been a topic of increasing interest for some time. The future of communication and information processing technologies depends on the use of nanometric and submicrometer integration as an essential tool.[2] Theoretical studies of the electronic conductance through nanometric-sized systems have already been carried out, including studies about their relationship with quantization and localization phenomena,[3,5,4,6–11] as well as their mechanical properties.[12–15]

With the advent of the scanning tunneling microscope (STM) (Ref. 16) and several related techniques, it became possible to study with extreme accuracy the transition from tunnel to contact regimes when two metallic electrodes (tip and sample) are approached. Since then, the STM has been widely used to study the phenomenon of conductance quantization (CQ). This was usually performed by driving a STM tip into a metallic sample and then pulling it out. During this process a nanowire is formed, making it possible to measure both electrical[15,17–19] and mechanical[20,21] properties. Conductance experiments have been performed with the mechanically controllable break junction technique[22–25] as well. Switching behavior has been also induced between tunneling and ballistic transport regimes by repeatedly bringing a sharpened nickel wire into contact with a gold surface.[26] These approaches conclude that, at low and high temperature, CQ occurs for several metallic species forming the contact.

Recently,[27] it has been found that the same quantization features appear in conductance experiments where two macroscopic wires are placed in contact, and the formation and breakage of the contacts is produced by making them vibrate. With this simple experimental technique, CQ has been observed for a wide variety of metallic macroscopic contacts under different environments [air, liquids, and ultrahigh-vacuum (UHV)]. These results, revealing the quantum nature of the conductance at the latest stages of the contact breakage, and obtained with the use of macroscopic electrodes, are indistinguishable from those obtained with other experimental techniques based on the control (via piezodisplacement techniques) of the separation of a sharp electrode. This proves that, independently on the initial contact area, at the latest stages of the breakage of a metallic contact, only a small bridge of nanometric dimensions (nanowire) is present. This process is probably due to the formation of nanoscopic threads at the last stages of the contact thin-out process; only one remains at the very end.

In the present paper we analyze more thoroughly the contact formed between two macroscopic wires using piezodisplacement techniques based on STM methods. We have been able to stabilize these nanometric-sized contacts during time scales three orders of magnitude (several hours) higher than previously reported measurements, characterizing its electronic behavior with unprecedented accuracy. We observe and study the nonlinear contribution to the *I-V* characteristic curves. Interesting statistical results on nanocontacts formed with STM are presented. A statistical analysis of the length of the first conductance plateau provides information about the correlation between force jumps due to atomic rearrangements and conductance jumps due to the change of the number of electronic levels in the constriction.

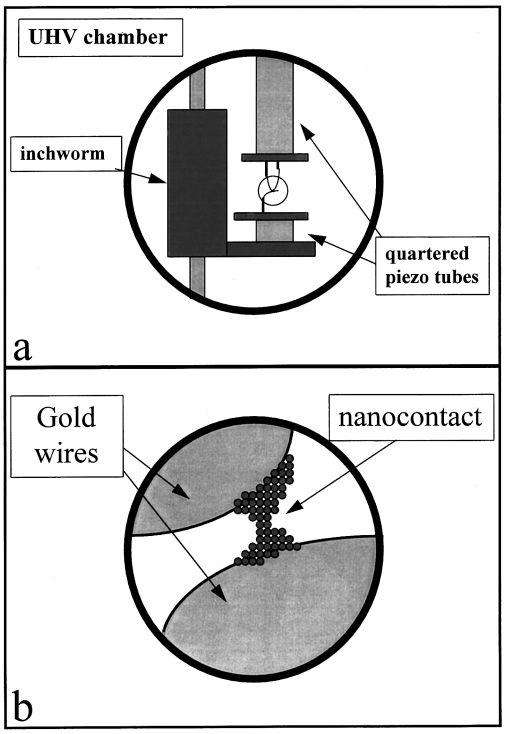

FIG. 1. (a) Experimental setup used to study the nanowire formation between macroscopic metallic electrodes in UHV at RT. (b) Schematic representation of the last stages of the contact breakage.

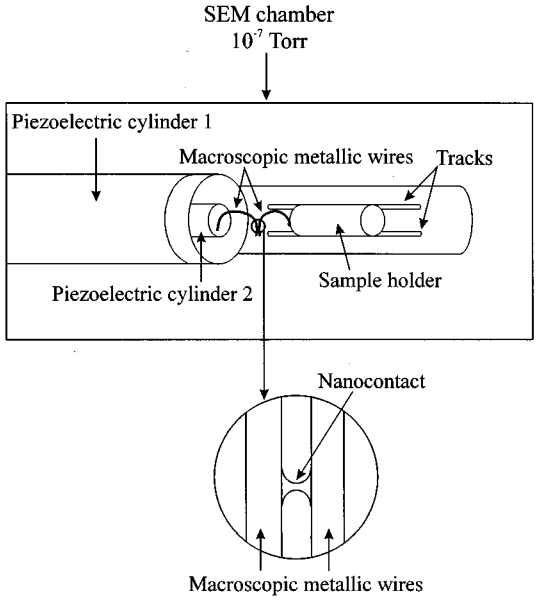

FIG. 2. Experimental setup used to visualize contacts between macroscopic metallic electrodes inside a scanning electron microscope (SEM).

II. DESCRIPTION OF THE EXPERIMENTAL SETUPS

In order to achieve control on the formation of nanocontacts, we used three different approaches. The first one corresponds to a conventional homemade STM setup, where the current flowing through the contact, during a tip indentation-retraction cycle, is continuously monitored with a current-voltage converter connected to a digital oscilloscope. With this setup, and driving the Z piezo with a triangular wave, several thousands of current decay curves (representing nanocontact breaking processes) can be measured in an hour. This huge amount of data improves previous statistical analysis of conductance curves, making it possible to build histograms with up to 1 000 000 single measurements.

Our second setup is schematically depicted in Fig. 1(a). In this configuration we tried to obtain maximum control of the formation of nanocontacts between two macroscopic wires. We placed two macroscopic metallic wires (having diameters larger than 100 μm) within an UHV chamber (with a typical pressure of 10^{-10} Torr). The separation between the macroscopic wires [enclosed by a circle in Fig. 1(a)] is controlled by a commercial inchworm and conventional STM piezoelectrics, which allows us to control the movement along the z direction, whereas it is possible to control vertical and lateral displacements (from Å to cm) with the combined use of two quartered piezotubes and a step motor. This UHV system has been suitably isolated from external mechanical vibrations. Previous to the measurements, both wire surfaces were cleaned, heating the wires up to 600 °C in UHV. All the experimental data presented in this work have been acquired at room temperature (RT).

A third setup is shown in Fig. 2, where the approach and separation processes between two macroscopic metallic wires are controlled with piezoelectric actuators. The setup is placed inside a scanning electron microscopy (SEM) chamber, making it possible to visualize the different stages of the formation and breaking of the metallic contacts. These studies are carried out under normal SEM vacuum conditions (10^{-7} Torr). Our SEM investigations include the characterization of the chemical composition of the contact region with an energy dispersive x-ray spectrometer (EDX).

Independently of the setup (under UHV or in air) the conductance measurement has been performed with two different techniques. One measures the current through the contact with a current-voltage (I-V) converter with 10^5 gain, 1-μs rise time, and a 3-μs settling time. The other is even simpler; the current through the contact is measured as a voltage drop through a 1-kΩ resistance placed in series with the contact. Both measurement techniques give identical conductance results.

III. CONDUCTANCE MEASUREMENTS

Figure 3 displays three nanowire conductance measurements performed under different experimental conditions. Figure 3(a) shows a typical conductance experiment obtained with a homebuilt STM at RT and in air with a gold tip and a gold sample. The stepped behavior of the conductance is well defined. Figure 3(b) shows a conductance decay measurement when two macroscopic gold wires (150-μm diameter, and 99.9% purity) in UHV at RT are separated, breaking the contact. This experiment has been performed within the UHV chamber described in Fig. 1(a). Displacement control in the nanometer range allows us to bring the electrodes into contact, recording simultaneously the current flowing through them. Once the contact is established, the electrode displacement is reversed and the formation and later elongation of the nanoneck [see Fig. 1(b)], breaking eventually,

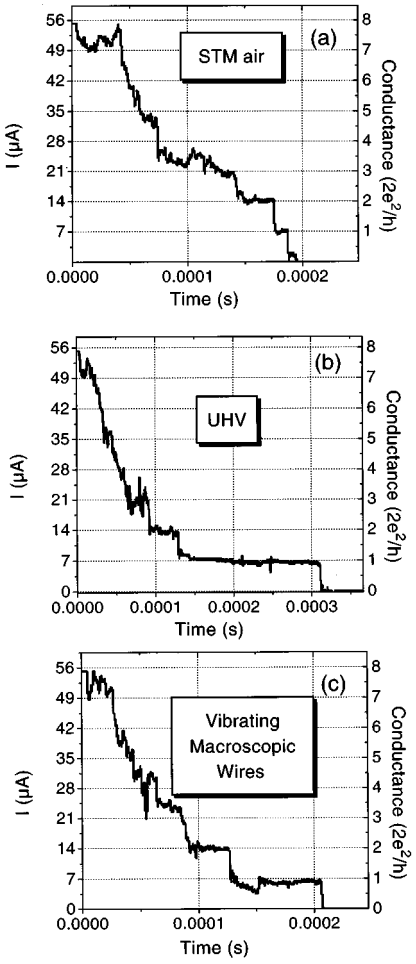

FIG. 3. Examples of contact breakage conductance experiments using different experimental setups: (a) STM in air, (b) UHV chamber depicted in Fig. 1 and, (c) vibrating macroscopic wires. The potential difference between electrodes is 90.4 mV in all cases.

appears as a change in the conductance in well-defined steps corresponding to the $2e^2/h$ quantized value. For the sake of comparison, Fig. 3(c) displays a conductance experiment obtained with a very simple setup: two macroscopic gold wires, 0.6 mm in diameter, vibrating close to the contact position after a mechanical perturbation. During the separation process there is clear evidence of the formation of nanocontacts with marked conductance quantization features.[27]

Notice that there are no substantial differences among curves obtained with the different approaches shown in Fig. 3, indicating that the conductance quantization is a rather general phenomenon associated to the breakage of macroscopic and microscopic contacts. To illustrate this point further, we have performed a statistical analysis of the conductance using a huge number of STM conductance measurements, building the corresponding conductance histogram. This histogram, obtained from 18 000 consecutive conductance curves obtained with a STM setup (gold tip and gold sample at RT) is shown in Fig. 4. This curve has been obtained without discarding any conductance curve measurement, avoiding any kind of *a priori* argument to build the histogram. This proves the massive production of nanowires with CQ behavior.

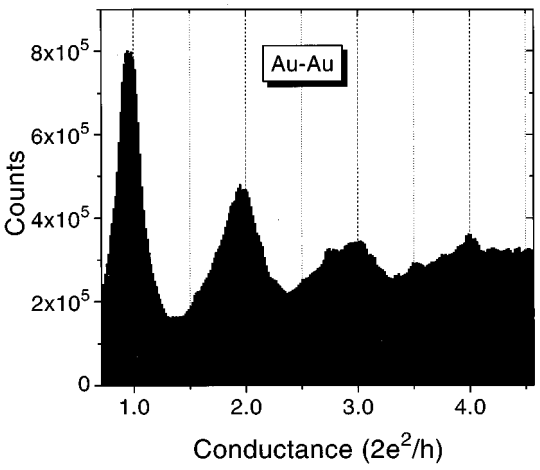

FIG. 4. Histogram of conductance values built with 18 000 consecutive gold contact breakage experiments. The experiment is performed in a STM or RT in air, with a potential difference between electrodes of 90.4 mV. The electrodes approach and separate at 89 000 Å/s.

The possibility of using macroscopic metallic wires to study the CQ opens attractive possibilities from the experimental point of view. For instance, it is possible to study the formation of nanocontacts in liquid systems, driving a liquid metal (mercury or liquid tin) in and out of a metallic tip until the formation of a contact. Figure 5 schematically depicts this experimental setup. In Fig. 6(a) we show conductance measurements for mercury nanocontacts, where clear conductance steps appear when driving the tip into contact with the liquid metal. Similar characteristics are obtained when measuring the conductance for liquid tin (at 300 °C), as shown in Fig. 6(b). In general, we find that liquid contacts present fewer plateaus than those found in solid metallic contacts. However, these plateaus are more pronounced. These experiments indicate that liquid systems present conductance characteristics similar to those of metallic solid systems at the nanometer scale.

IV. HIGH STABILITY NANOCONTACTS AND SWITCHING BEHAVIOR

As shown in Sec. III, when two Au wires, initially separated, are brought into contact after a controlled approxima-

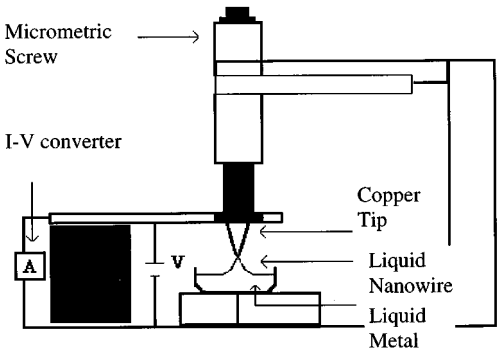

FIG. 5. Scheme of the experimental setup for conductance quantization studies in liquid metals. A micrometric screw is used to control the tip displacement.

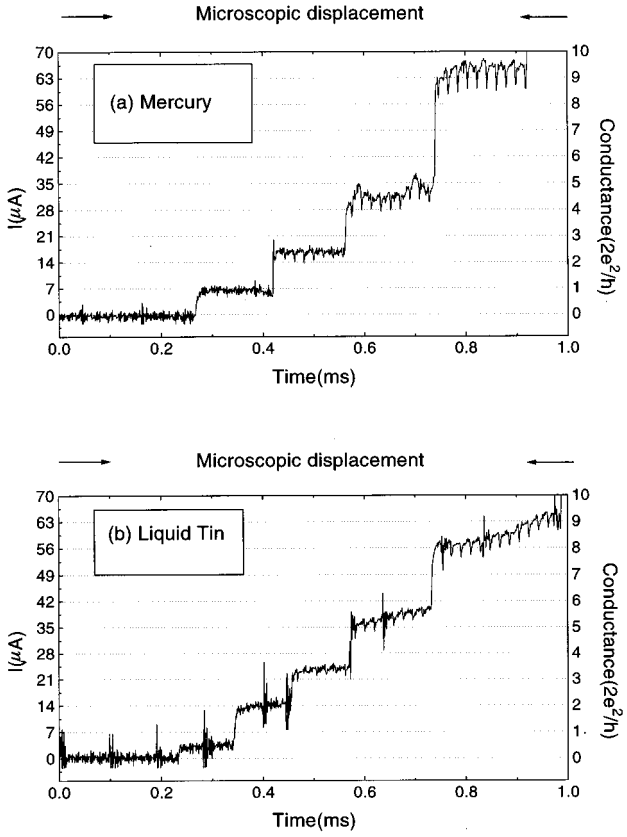

FIG. 6. Conductance experiments showing the evolution of the current and the conductance at the first stages of the formation of a liquid metal contact. The contact forms between a cooper wire and (a) mercury (at room temperature) and (b) liquid tin (at 300 °C). The applied bias voltage between tip and the metallic liquid reservoir is 90.4 mV.

tion between them, it is possible to form a small contact corresponding to a relative low number of eigenstates through which the electronic ballistic transport takes place. In this section we describe how the UHV setup is used to study the evolution of the current during the approach and separation of two macroscopic wires. Once the contact is established, we observe that it remains stable for a long time (up to hours), and that, we need large inchworm displacements ($\approx 1\,\mu$m) to break it. In our opinion, the high stability is due to two extrinsic factors: the excellent mechanical isolation of the UHV chamber, and the intrinsic isolation provided by the configuration of the macroscopic electrodes, where one electrode is a wire free to bend [see Fig. 1(a)]. This is an important factor, since we have observed that contacts formed between rigid wires are less stable.

At constant voltage, the current flowing through the contact is continuously monitored during all approach and retraction processes. On approaching the wires to contact inchworm steps, we are able to reach a position very close (about nm) to the formation of a nanocontact. Under this situation we observe conductance switching between 0 and 1 (in units of $2e^2/h$), as shown in Fig. 7(a). This switching behavior has also been observed between 0 and 2 conductance channels [Fig. 7(b)]. Notice that the time scale on which this phenomenon occurs is of the order of seconds, and that these

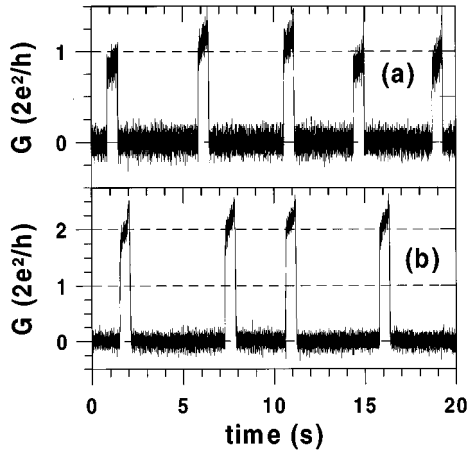

FIG. 7. Switching behavior observed in gold contacts in UHV at RT. (a) Transitions between 0 and one quantum channels. (b) Transitions between 0 and two quantum channels.

measurements are performed at RT. A similar switching behavior has been observed using a Ni tip and a Au sample in a STM configuration at 4.6–8.6 K, on the ms time scale.[26]

After this switching behavior, an inchworm step usually produces the formation of a stable contact involving a huge number of conduction channels. In our experiments, the current window is limited to 140 μA. The current versus displacement characteristics measured in the excursions in and out of the contact are hysteretic, similarly to what has been observed in STM experiments. This hysteresis made it somehow difficult to stabilize the current inside the experimental window, although, after several approaching-separation processes using smaller inchworm steps (2 nm) and quartered piezo tubes, we finally managed to obtain a stable current. Concerning the approach procedure, it should be mentioned that the lower the voltage difference between the macroscopic wires, the lower the hysteresis in the contact–noncontact transitions, and the easier to stabilize the current within the experimental window.

Once stabilized, we observed a constant current for several hours. This corresponded to a single metallic contact involving a few conductance levels. This means we improve the stability reached by standard STM techniques by more than three orders of magnitude[15,17–19] at RT.

In general, only external sources of mechanical noise (for instance, a small inchworm displacement (2 nm), door bangs, etc.) change the conductance once stabilized. In these cases, either the contact breaks totally, or the conductance presents a clear jump between two quantized values, indicating a change in the contact section. In Fig. 8 we display the time evolution of the current for three selected nanocontacts, with a clear evidence of this kind of transitions due to mechanical vibrations. Figure 8(a) shows a contact initially stabilized at $G=3G_0$, followed by a jump to $G=G_0$ due to a door bang in the lab. Figure 8(b) presents a more marked jump between 22 and six conduction channels. This was due to a step close to the UHV chamber. In Fig. 8(c) we show two conductance transitions; one from nine to five, and a second one from five to seven conductance channels. Notice the time scale in Fig. 8.

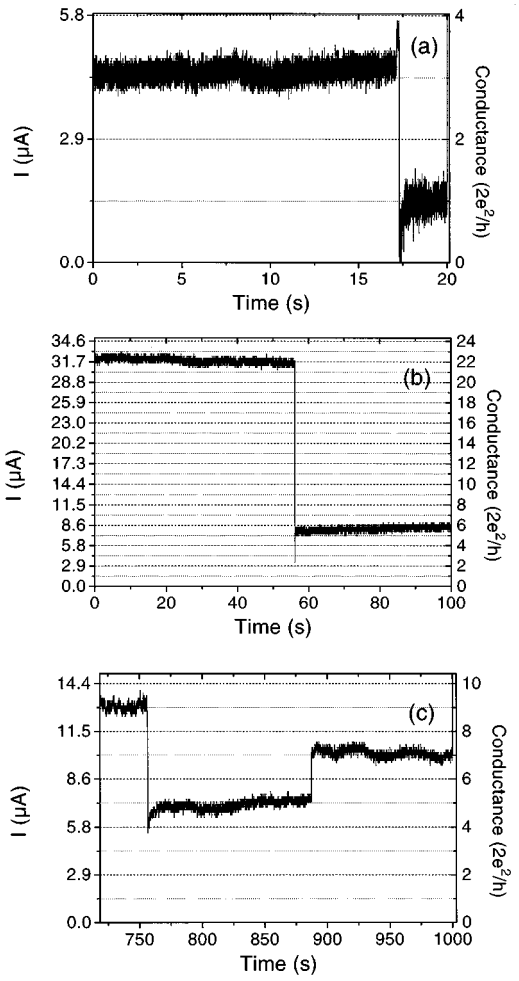

FIG. 8. Conductance transitions due to mechanical instabilities for gold nanocontacts in UHV at RT. (a) Transition from three to one quantum channels. (b) Transition from 22 to six quantum channels. (c) Transition from nine to five and to seven quantum channels.

V. INTENSITY-VOLTAGE CHARACTERISTICS

High stability nanocontacts allows the measurement of their *I-V* characteristic curves. A triangular potential difference is applied to the contact (see the inset in Fig. 9), with a time period ranging from 0.1 to 50 s, recording the current simultaneously. As an example, in Fig. 9 we present experimental current data as a function of time for a gold-gold nanocontact with a conductance corresponding to four quantum channels. There are two features we would like to stress. First, the static value of the current prior to the ramp in voltage corresponds in this case to four quantum channels. Second, notice the current nonlinearity for values of the applied voltage larger than about 100 mV.

We have performed extensive measurements and analysis of the *I-V* characteristic dependence on the quantum channel number. In Fig. 10 we plot a series of *I-V* characteristic curves obtained for the same contact at different stages (different quantized values) of the pulling process. All these curves correspond to different breaking stages of a single nanoneck. At a first glance, the *I-V* characteristic curves present a well-defined linear behavior for contacts having

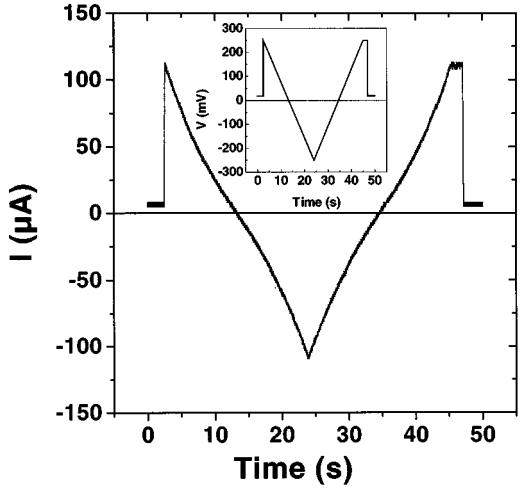

FIG. 9. Time evolution of the current through a nanocontact when the voltage ramp shown in the inset is applied. Note the time scale of the experiments, the nonlinearity of the current, and the fact that current returns to exactly the same value after the voltage ramp. The dynamical conductance at zero bias corresponds to four quantum channels.

large conductances, whereas for contacts involving only few conductance channels nonlinear effects become evident. In all cases, the dynamical conductance (the slope of the *I-V* characteristic at zero bias) agrees within a few percent with the expected quantized conductance value $[n\times(2e^2/h)]$.

We have fitted the measured current dependence on the applied voltage to the expression

$$I(V)=I_L(V)+I_{\mathrm{NL}}(V)=a_1\mathrm{V}+a_2\mathrm{V}^2+a_3\mathrm{V}^3, \qquad (1)$$

where $I(V)$ is the value of the current in μA, V is the applied voltage in volts, and, I_{L} and I_{NL} are the linear and no-linear contributions, respectively. This nonlinear component is represented in Fig. 11 for some of the *I-V* curves shown in Fig. 10 (one, two, three, and six channels), showing that the nonlinear character does not depend strongly on the

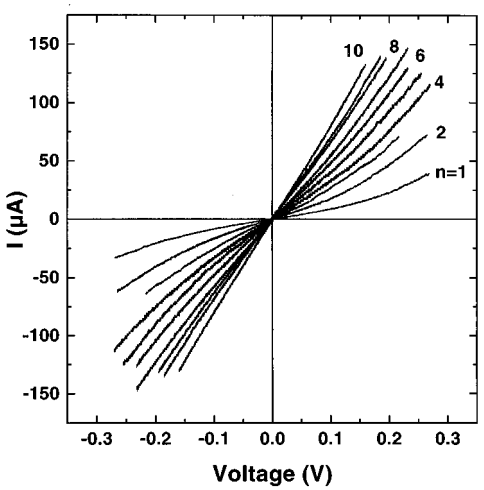

FIG. 10. Nonlinear *I-V* characteristics for different quantum channels, measured as the dynamical slope at zero bias, denoted by *n*.

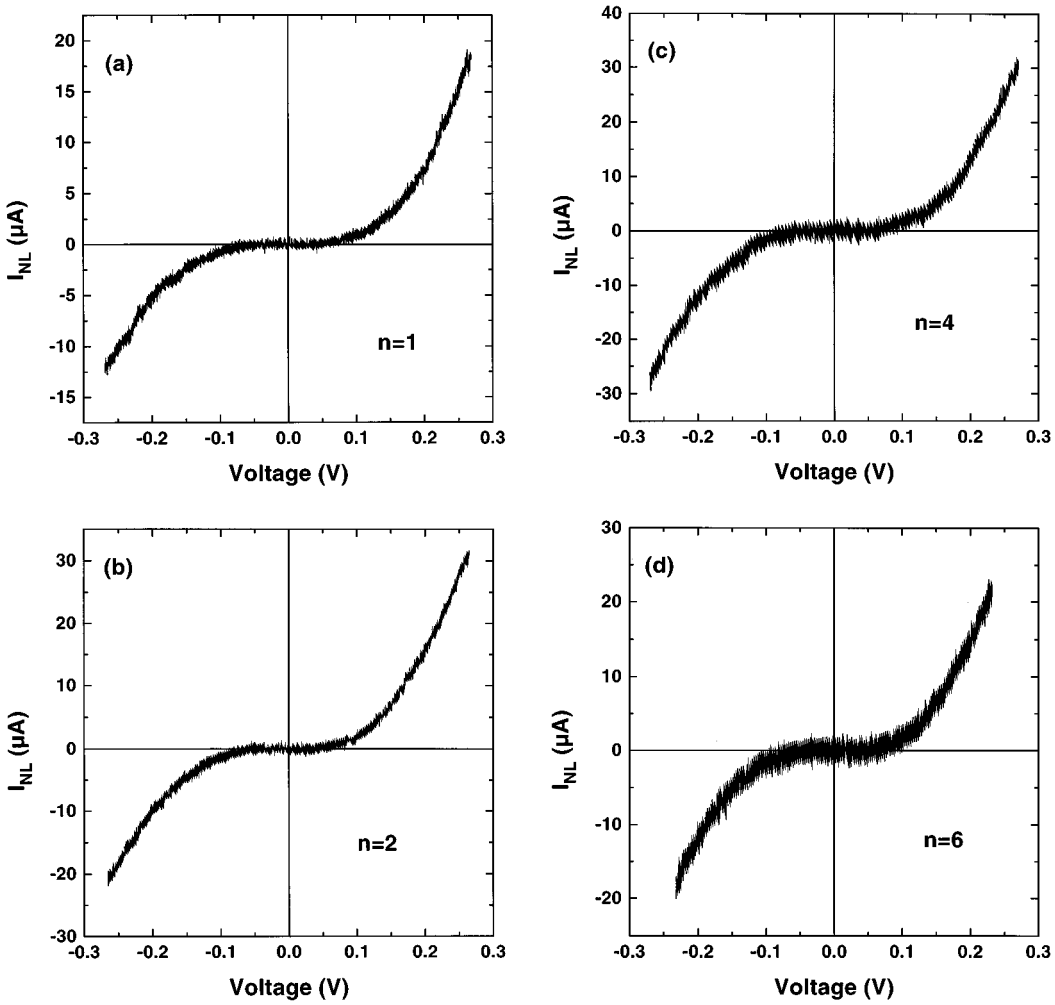

FIG. 11. Nonlinear part of the *I-V* characteristic of gold nanowires in UHV for (a) $n=1$, (b) $n=2$, (c) $n=4$, and (d) $n=6$ quantum channels.

conductance channel. In Fig. 12 we plot the coefficients a_1, a_2, and a_3 for another series of measurements. As observed, $a_2 \ll a_3$ with a_3 nearly independent on the conductance channel. We find that $a_3 = 1500 \pm 150$ (averaging over all the measurements). These considerations indicate a more cubiclike behavior of the nonlinear component of the *I-V* curve. Notice that the *I-V* curves do not reflect the existence of changes in the slope with a value of e^2/h as reported in STM measurements using a tungsten tip and a gold substrate.[28]

In order to analyze in detail the nonlinear component of the *I-V* characteristic curves, we have assumed that $I_{NL}(V)$ can be fitted to a potential law pV^q. Figure 13 shows this exponent q for a wide set of measurements. Notice that the value of the exponent q spreads out over a range of values between 2 and 4; however, a statistical analysis of these data reveals (see the inset in Fig. 13) a more cubiclike behavior, being the average exponent $q \approx 2.93 \pm 0.15$.

Therefore, since the nonlinear component is almost independent on the nanocontact conductance, whereas the linear part obviously increases with the number of propagating channels, the linear behavior quickly becomes dominant, and, only for contacts with low conductance values, the nonlinear contribution becomes noticeable. The most plausible origins of this behavior are connected with Coulomb blockade phenomena in small conducting systems, or the special conducting properties of Luttinger liquids.[29]

VI. NANOWIRE VISUALIZATION

Conductance measurements provide useful insight when studying nanocontacts and, as mentioned above, point out to the formation of connective necks between the electrodes. A direct observation of the contact structure is then of considerable interest. In order to show the existence of these nanocontacts, we have carried out a set of experiments where the macroscopic electrodes are approached with piezocontrol inside a SEM. After a contact is produced, surface modifications appearing at the contact region when separating the electrodes are visualized, and the setup is shown in Fig. 2. In this series of experiments silver wires, 0.25-mm diameter, have been used.

Our SEM analysis reveals the existence of small nanocontacts formed between the macroscopic metallic electrodes. We observed many of these nanostructures in Ag contacts, presenting both irregular and smooth shapes. The SEM resolution only allows the visualization of the nanoneck at early

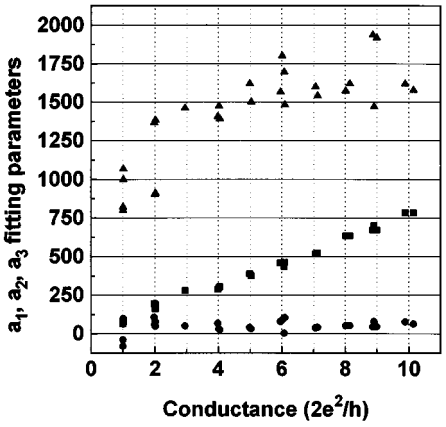

FIG. 12. Third-degree polynomial fitting results for several *I-V* curves for gold nanowires in UHV at RT. The linear coefficient a_1 is represented by solid squares, the quadratic a_2 by solid circles, and the cubic a_3 by solid triangles.

evolution stages on breaking the contact. However, the obtained images point unambiguously to the formation of a connective neck between electrodes. In Fig. 14(a) we present one SEM micrograph of a silver nanocontact. The image shows a contact with a length of 800 nm, and a minimum diameter section of ≈300 nm. We have performed EDX chemical analysis in this metallic bridge formed between macroscopic wires, detecting a large Ag signal [Fig. 14(b)]. No traces of contaminants like carbon, oxygen, etc. were found, indicating that the nanocontact material comes from the macroscopic wire electrodes. Similar nanocontact images have been found with Au and Cu electrodes. This series of experiments clearly demonstrates the existence of nanocontacts appearing when two macroscopic metals separate. Preliminary transmission electron microscopy (TEM) images carried out in our laboratory reveal also the existence of these nanocontacts down to width scales of the order of 1–2 nm.

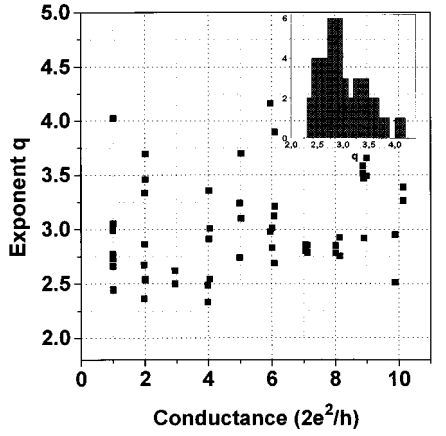

FIG. 13. Power-law fitting result of the nonlinear part of several *I-V* characteristics of gold nanowires in UHV at RT. The inset shows the histogram of the exponents, revealing the cubic dependence of this nonlinear part.

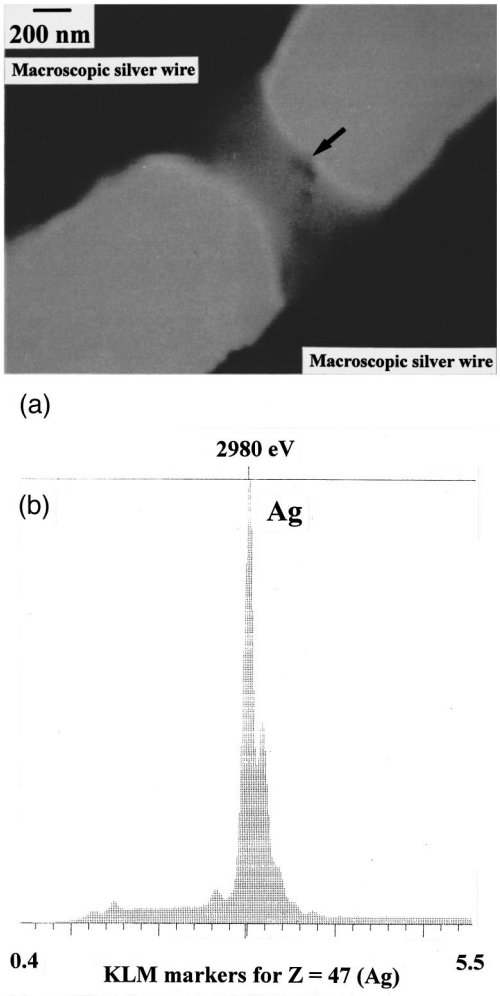

FIG. 14. (a) SEM image showing a nanocontact ≈300-nm width between macroscopic silver wires. (b) EDX chemical analysis performed on this metallic ''bridge'' with an ultrathin window energy x-ray spectrometer showing a large Ag signal. No signal from contaminant elements was detected. Small peaks are due to the sample holder. The probe size used during this analysis was ≈200 nm.

VII. DISTRIBUTION OF STATES AT THE NANOWIRE CONSTRICTION

In the previous sections we analyzed some properties concerning nanocontacts formed between macroscopic electrodes, showing that our technique provides very stable nanocontacts, and that *I-V* characteristics can be measured over long-time scales. In addition, we demonstrated that these nanostructures are present when a macroscopic contact breaks, and that they exhibit well-marked conductance features. In this section, we address a different problem. We analyze statistically the length of the conductance plateaus. To carry out these measurements, we have used the STM setup, with controlled electrode approach and separation, at 89 000 Å/s, at RT and in air. We stored 3200 curves, characterized by well-defined quantized conductance steps (those conductance curves with clear plateaus at $G/G_0=1,2,3$). Since the separation speed is known, we determine the elongation corresponding to each plateau, and analyze statistically the distribution of such lengths. In Fig. 15 the histogram of elongations corresponding to the first conductance

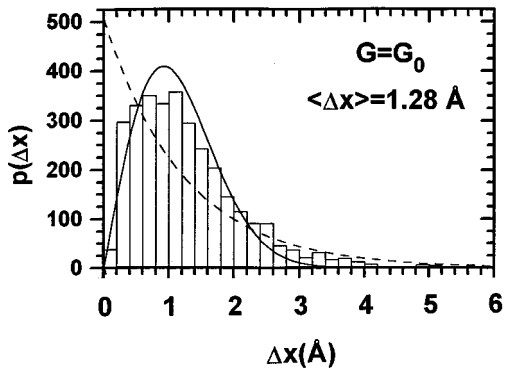

FIG. 15. Histogram showing the distribution of the duration of the first conductance plateau for contacts formed between a gold macroscopic wire (1-mm diameter) and a gold plate, at RT and with an electrode separation speed of 89 000 Å/s. The solid line represents a Wigner distribution fit with parameter $a=2.36\pm0.09$ (see text). The dashed line is a fit to the Poisson distribution with a fitting parameter $b=0.81\pm0.04$.

plateau is displayed. It is clear that the elongation distribution is very broad. The average value of the distribution shown is 0.13 nm, close to the gold interatomic distance. This average value decreases to 0.11 nm for the second conductance quantization level, and to 0.10 nm for the third conductance quantized level.

These results are at variance with previous experiments based on STM setups,[20,21] in which atomic rearrangements during nanowire pulling processes are detected at well-defined elongation values, with narrow length distributions. Furthermore, the dependence of the elongation distribution (or elapsed times) on the conductance value seems to be consistent with conductance jumps caused by the decrease of the nanocontact section under a uniform pull, instead of conductance jumps caused by atomic rearrangements.

To show that this kind of histogram can be interpreted in terms of the separation between electronic levels of the nanoneck, we propose a very simple model. Consider a cylindrical neck with volume $V=S\times l$ (S being the neck section and l its length), and assume that the electrodes separate with a constant velocity (in our experiments a linear voltage ramp drives the piezo). The section varies as $S\propto 1/l$ assuming a constant neck volume.[15] For the two-dimensional section, the energy of the last allowed electronic level is roughly $E\propto 1/S$. Thus, in this simple model, the variation of the energy level with length is $E\propto l$. In other words, by measuring conductance plateaus (the length between two subsequent conductance jumps), we measure the distribution of the separation in energies of nearest-neighbor quantum levels (ΔE). This simple model also predicts that the higher the conductance value the shorter the elapsed time in its associated plateau, as experimentally observed. If the results shown in Fig. 15 are interpreted in terms of the proposed model, the distribution can be viewed as the distribution of the energy jumps between two consecutive levels. Figure 15 would then represent the distribution of energy differences between the first and second electronic eigenstates formed within the nanowire during the elongation process. We have fitted length histograms, like the one presented in Fig. 15, to different functions in order to study them from this point of view. We have used a Wigner distribution (solid line in Fig. 15)

$$P(x)=a(x/2)\exp(-a(x/2)^2), \tag{2}$$

where a is a fitting parameter. This law is followed by the distribution of energy changes in quantum chaos problems (as the Stadium[30] and Sinai's billiard[31] problems). On the other hand, we know that for integrable systems, with more than one degree of freedom, the distribution should be described by a Poisson-like (dashed line in Fig. 15) law[32]

$$P(x)=b\exp(-bx), \tag{3}$$

b being the corresponding fitting parameter. In order to determine the parameters a and b associated with both distributions (Wigner and Poisson), we fitted our data to the cumulative probability $N(x)=\int_0^x P(x)dx$, since $N(x)$ has a smooth behavior and does not depend on the bin size.

Clearly, the experimental distribution does not correspond to the Poisson type, as expected for circular constriction sections.[30,32] However, the Wigner distribution fits well the experimental histogram shown in Fig. 15. This fact supports the idea that the energy-level spectrum of the nanocontacts corresponds to that of a quantum chaotic system. Furthermore, the plateau length histogram shows a broad distribution of lengths, in contrast with the force jumps[12] that are at constant length. Our data then suggest that the conductance steps are not only due to sudden changes in cross section, but also to the pinching off of states at the constriction in a continuous way.[14,19]

VIII. CONCLUSIONS

Summarizing, electrical and mechanical properties of metallic nanocontacts have been studied with microscopic and macroscopic electrodes and different experimental setups. All involve the controlled approach and separation between metallic electrodes. Controlled experiments with gold wires in vacuum conditions are presented. The nanocontacts formed between macroscopic electrodes can be visualized by SEM. These nanocontacts exhibit a high stability, allowing measurements of currents flowing through nanocontacts during hours. These high-stability features have been used to measure the I-V characteristic curves, showing the importance of nonlinear effects in contacts involving few conduction channels. The study of these I-V curves opens theoretical challenges that probably will be understood in terms of electron-electron interaction effects. The distribution of plateau lengths, and the corresponding conductance steps and force jumps, indicate that these two events do not correspond biunivocally.

ACKNOWLEDGMENTS

This work was supported partially by the Spanish DGICyT PB94-0151 and CICyT MAT94-1456-CE projects, and the HCM, BRITE-EURAM, and ESPRIT programmes from the European Union. P.G.-M. received a grant from the FPI program of the CAM (Spain).

[1] B. J. van Wees, H. van Houten, C. W. J. Beenakker, J. G. Williamson, L. P. Kouwenhoven, D. van der Marel, and C. T. Foxon, Phys. Rev. Lett. **60**, 848 (1988); D. A. Wharham, T. J. Thornton, R. Newbury, M. Pepper, H. Ahmed, J. E. F. Frost, D. G. Hasko, D. C. Peacock, D. A. Ritchie, and G. A. C. Jones, J. Phys. C **21**, L209 (1988).

[2] Joint European-American-Japanese Conference on Future Information Technologies, Helsinki, Finland, 1995 (unpublished).

[3] P. W. Anderson, Phys. Rev. **109**, 1492 (1958).

[4] N. D. Lang, Phys. Rev. B **36**, 8173 (1987).

[5] R. Landauer, J. Phys. Condens. Matter **1**, 8099 (1989).

[6] N. García and L. Escapa, Appl. Phys. Lett. **54**, 1418 (1989); N. García (unpublished).

[7] For the 2D electron gas, see the review by C. W. J. Beenaker and H. V. Houten, in *Solid State Physics*, edited by H. Ehrenreich and D. Turnbull (Academic, New York, 1991), Vol. 44.

[8] E. Kander, Y. Imry, and U. Sivan, Phys. Rev. B **41**, 12 941 (1990).

[9] R. García and N. García, Surf. Sci. **251/252**, 408 (1991).

[10] J. Torres, J. I. Pascual, and J. J. Sáenz, Phys. Rev. B **49**, 16 581 (1994); E. N. Bogachek, A. M. Zagoskin, and I. O. Kulik, Fiz. Nizk. Temp. **16**, 140 (1990) [Sov. J. Low Temp. Phys. **16**, 796 (1990)].

[11] P. García-Mochales, P. A. Serena, N. García, and J. L. Costa-Krämer, Phys. Rev. B **53**, 10 268 (1996); T. N. Todorov and G. A. D. Briggs, J. Phys. Condens. Matter **6**, 2559 (1994).

[12] U. Landman, W. D. Luedtke, N. A. Burnham, and R. J. Colton, Science **248**, 454 (1990); U. Landman and W. D. Luedtke, J. Vac. Sci. Technol. **9**, 414 (1991).

[13] T. N. Todorov and P. Sutton, Phys. Rev. B **70**, 2138 (1992).

[14] A. M. Bratkovsky, A. P. Sutton, and T. N. Todorov, Phys. Rev. B **52**, 5036 (1995).

[15] J. I. Pascual, J. Méndez, J. Gómez-Herrero, A. M. Baró, N. García, U. Landman, W. D. Luedtke, E. N. Bogacheck, H.-P. Cheng, Science **267**, 1793 (1995).

[16] G. Binnig, H. Rohrer, Ch. Gerber, and E. Weibel, Phys. Rev. Lett. **49**, 57 (1982).

[17] J. I. Pascual, J. Méndez, J. Gómez-Herrero, A. M. Baró, N. García, and V. T. Binh, Phys. Rev. Lett. **71**, 1852 (1993).

[18] L. Olesen, E. Laegsgaard, I. Stensgaard, F. Besenbacher, J. Schiotz, P. Stoltze, K. W. Jacobsen, and J. K. Norskov, Phys. Rev. Lett. **72**, 2251 (1994).

[19] M. Brandbyge, J. Schiotz, M. R. Sorensen, P. Stoltze, K. W. Jacobsen, J. K. Norskov, L. Olesen, E. Laegsgaard, I. Stensgaard, and F. Besenbacher, Phys. Rev. B **52**, 8499 (1995).

[20] N. Agraït, J. G. Rodrigo, and S. Vieira, Phys. Rev. B **47**, 12 345 (1993).

[21] N. Agraït, G. Rubio, and S. Vieira, Phys. Rev. Lett. **74**, 3995 (1995).

[22] C. J. Muller, J. M. van Ruitenbeek, and L. J. de Jongh, Phys. Rev. Lett. **69**, 140 (1992).

[23] J. M. Krans, C. J. Muller, I. K. Yanson, Th. C. M. Govaert, R. Hesper, and J. M. van Ruitenbeek, Phys. Rev. B **48**, 14 721 (1993).

[24] J. M. Krans, C. J. Muller, N. van der Post, F. R. Postma, A. P. Sutton, T. N. Todorov, and J. M. van Ruitenbeek, Phys. Rev. Lett. **74**, 2146 (1995). See the Comment by L. Olesen *et al.*, Phys. Rev. Lett. **74**, 2147 (1995).

[25] J. M. Krans, J. M. van Ruitenbeek, V. V. Fisun, I. K. Yanson, and L. J. de Jongh, Nature (London) **375**, 767 (1995).

[26] D. P. E. Smith, Science **269**, 371 (1995).

[27] J. L. Costa-Krämer, N. García, P. García-Mochales, and P. A. Serena, Surf. Sci. **342**, L1144 (1995).

[28] V. V. Dremov and S. Yu. Shapoval, Pis'ma Zh. Éksp. Teor. Fiz. **61**, 321 (1995) [JETP Lett. **61**, 337 (1995)].

[29] C. L. Kane and M. P. A. Fisher, Phys. Rev. B **46**, 15 233 (1993); D. L. Maslov and M. Stone, *ibid.* **52**, R5539 (1995).

[30] S. W. McDonald and A. N. Kaufman, Phys. Rev. Lett. **42**, 1189 (1979); Phys. Rev. A **37**, 3067 (1988) and references therein.

[31] O. Bohigas, M. J. Giannoni, and C. Schmit, Phys. Rev. Lett. **52**, 1 (1983).

[32] M. V. Berry and M. Tabor, Proc. R. Soc. London **356**, 375 (1977).